AIAA JOURNAL
Vol. 39, No. 3, March 2001

Interaction of Vortex Breakdown with an Oscillating Fin

Ismet Gursul*
University of Bath, Bath, England BA2 7AY, United Kingdom
and
Wensheng Xie†
University of Cincinnati, Cincinnati, Ohio 45221-0072

The interaction of vortex breakdown with an oscillating fin was investigated by flow visualization and velocity measurements to understand the effects of aeroelastic deflections on fin buffeting. For frequencies lower than a cutoff frequency, the response of vortex breakdown location is quasi periodic, and the amplitude of the variations of breakdown location decreases with increasing frequency. For frequencies higher than the cutoff frequency, vortex breakdown does not respond to the fin oscillations. These observations suggest that the dynamic response of breakdown location to an oscillating fin is similar to that of a low-pass filter. For different locations of the fin with respect to the vortex, similar amplitude responses were found. This result can be used in the design of fins to prevent a feedback effect and coupling between the vortex breakdown and fin structure. A theoretical explanation of the experimental observations based on the wave propagation characteristics of the vortex flows is presented.

Nomenclature

AR	=	amplitude ratio
a	=	radius of Rankine vortex
b	=	semispan at trailing edge of delta wing
C_g	=	group velocity
c	=	chord length, phase speed
f	=	frequency
f_e	=	fin oscillation (excitation) frequency
k	=	axial wave number
n	=	azimuthal wave number
Re	=	Reynolds number
r	=	radial distance from vortex axis
S	=	power spectral density
s	=	local semispan
t	=	time
U_∞	=	freestream velocity
V	=	swirl velocity
W	=	axial velocity
x	=	chordwise distance from wing apex
x_{bd}	=	streamwise distance of breakdown location from the apex of the wing
$\bar{x}_{bd}$	=	time-averaged breakdown location
x'_{bd}	=	fluctuations of breakdown location
$(x'_{bd})_{rms}$	=	rms value of breakdown location
y	=	spanwise distance from wing root
y_f	=	spanwise location of the fin
z	=	distance above wing surface
α	=	angle of attack
Δt	=	sampling time interval
Δx	=	streamwise distance from the time-averaged breakdown location
θ	=	azimuthal angle
Λ	=	sweep angle
τ	=	time constant
ϕ	=	fin angle
Ω	=	angular velocity of Rankine vortex
ω	=	radial frequency

Received 19 February 2000; accepted for publication 15 September 2000.

*Reader in Aerospace Engineering, Department of Mechanical Engineering. Senior Member AIAA.
†Graduate Student, Department of Mechanical, Industrial, and Nuclear Engineering.

Introduction

A TYPICAL fighter aircraft performs maneuvers at high angle of attack. Separated vortical flows originating from delta wings, leading-edge extensions, and forebodies interact with fins and tails. Experimental evidence suggests that several unsteady flow phenomena may excite fins depending on angle of attack.[1] Vortex breakdown phenomenon is the most important source of fin buffeting, causing large structural vibrations and severe fatigue damage. The interaction of vortex breakdown with a fin is a complicated process affected by 1) the time-averaged breakdown location, which is determined by the pressure gradient set by the fin; 2) helical mode instability of the flow downstream of breakdown[2]; 3) quasi-periodic oscillations of breakdown location[3]; 4) distortion of incident vortex and vortex splitting[4–7]; 5) unsteady flow separation from the leading edge of the fin[7]; 6) possible coupling between the flow separation and vortex breakdown (with a feedback effect)[1,8]; and 7) aeroelastic deflections of the fin. Different aspects of fin buffeting have been previously investigated in above references and other studies.[9–13] However, the effect of aeroelastic deflections of the fin has not been investigated before.

An important aspect of the interaction of vortex breakdown with a fin is a possible feedback effect of the fin on the vortex breakdown location. Patel and Hancock[8] suggested a possible coupling between the flow separation over a rigid surface and vortex breakdown. This suggestion was investigated by studying the unsteady nature of breakdown location.[1] The time history of breakdown location obtained from flow visualization revealed certain dominant frequencies that are not observed for nonimpinging flows. Therefore, this may be an indication of a feedback effect on vortex breakdown. The physical mechanism of the feedback effect, if any, is not clear. One possible explanation is related to the wave propagation characteristics of the vortices. The disturbances generated at the leading edge of the fin may propagate upstream in the subcritical flow downstream of vortex breakdown. If the waves can propagate upstream through the vortex core, the flow is called subcritical. This definition is based on the time-averaged flow in columnar vortices. According to Leibovich,[14] the measured flows downstream of breakdown are subcritical.

In case of aeroelastic deflections of the fin, there may be similar feedback effect on vortex breakdown. It is well known that unsteady loads due to vortex breakdown excite the natural frequencies of the aircraft fin structure. Disturbances due to aeroelastic effects (surface deflections) may propagate upstream, resulting in large oscillations of breakdown location. In turn, these oscillations of vortex breakdown location may excite the fin and, hence, set up a limit-cycle oscillation due to the coupling between the vortex dynamics and the fin structure. The feedback effect of fin oscillations was not

considered by previous investigators, although the sensitive nature of vortex breakdown to small changes and the subcritical nature of the flow downstream of breakdown are well known.

The objective of this work is to study the effect of fin deflections on vortex breakdown with a simple experimental model. Aeroelastic deflections of the fin in the first bending mode will be simulated by forced oscillations of a rigid fin about a hinge because this mode of buffeting is the most dangerous. The main parameter is the frequency of the fin oscillations with a fixed amplitude.

Experimental Setup

Flow visualization and laser Doppler velocimetry (LDV) measurements were carried out over a delta wing. The experiments were performed in a water channel with a cross-sectional area of 61×61 cm. The turbulence level in the channel was 0.6%. To simulate aeroelastic deflections of the fin in the first bending mode, forced oscillations of a rigid fin about a hinge were used (Fig. 1). The delta wing model had a sweep angle of $\Lambda = 75$ deg and a chord length of $c = 203$ mm. The lee surface was flat, whereas the leading edges were beveled at 45 deg on the windward side. The thickness of the delta wing was 12.7 mm. The Reynolds number based on the chord length was around $Re = 4.1 \times 10^4$. The main dimensions of the fin are given in Fig. 1. The thickness of the fin was 5 mm. The leading edge of the fin was double beveled at an angle of 30 deg. The fin was attached to the delta wing by the mounting block near the trailing edge of the wing.

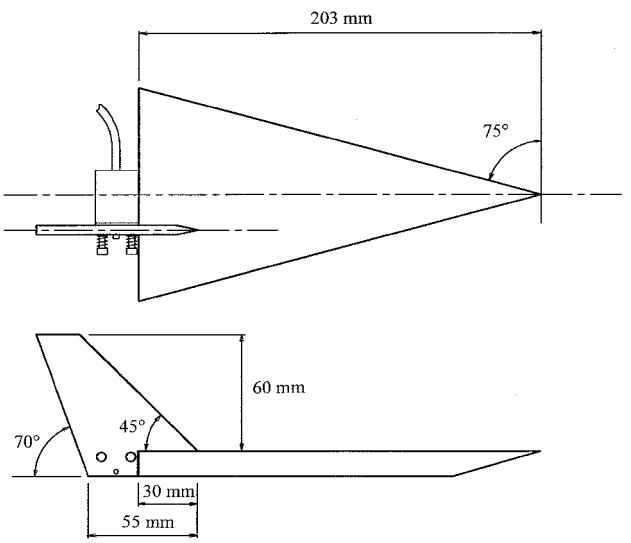

Fig. 1a Overview of delta wing-oscillating fin system.

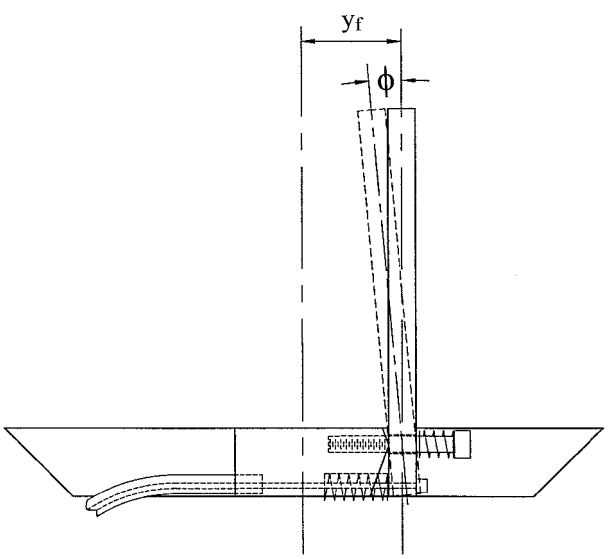

Fig. 1b Oscillating fin mechanism.

The deflection of the fin was achieved by pulling a bicycle brake cable, which was attached to the fin as shown in Fig. 1b. The fin was deflected out by pulling the cable, and the springs assured the fin motion in the opposite direction when the tension on the cable was released. The sheath of the cable was fixed to the mounting block. The other end of the cable was attached to the linkage of a crank arm mechanism (which was adapted from an existing pitching mechanism). A variable-speed dc motor and a speed controller were used to drive the mechanism. A displacement transducer was used to monitor the variation of the fin deflection angle. The maximum fin deflection angle was 10 deg.

Flow visualization of vortex breakdown was performed by injecting fluid with food coloring dye near the apex of the model. The motion of vortex breakdown location was recorded by a video system, which consisted of a video cassette recorder (at 30 frames/s resolution), a frame counter/window inserter, and a charge-coupled device camera with a zoom lens. The videotape recording of the motion was analyzed frame by frame. Computerized image processing techniques were not successful in attempts to detect vortex breakdown location. Consequently, the chordwise position of the breakdown location was determined directly by measuring the distance from the apex to the breakdown location on a video monitor screen. The breakdown was of the spiral type most of the time, as generally observed over delta wings. The location of breakdown was taken as the location where the streakline marking the core makes an abrupt kink to form a spiral. Defined as the point of the kink, the spiral-type breakdown was easy to determine. The uncertainty in breakdown location depends on the uncertainty in locating the breakdown, the reading uncertainty of scale on video images, and the magnification of the lens. The overall uncertainty in breakdown location was estimated to be $0.004c$. The time history of breakdown location is obtained for a total length of time record from $100c/U_\infty$ to $300c/U_\infty$ and with a sampling frequency of 3 frames/s (corresponding to a time resolution of $0.333c/U_\infty$).

The velocity was measured with a single-component LDV system operating in the back scattering mode. It consisted of a 10-mW HeNe laser, a Bragg cell for frequency shift, an integrated laser optics package, and a fiber optic cable. A correlation signal processor was used to analyze the data. The measurement volume size was about 0.08 mm in diameter and 0.65 mm in length. The measurement uncertainty for the mean velocity was estimated as 1%. The component of flow velocity parallel to the wing surface was measured at several points by traversing across the vortex core in the spanwise direction. Because the LDV system has the capability of measuring a single component of velocity, the swirl velocity component was measured separately by rotating the optical probe (therefore, measuring the velocity component normal to the wing surface). The component of flow velocity parallel to the wing surface was also measured in a crossplane.

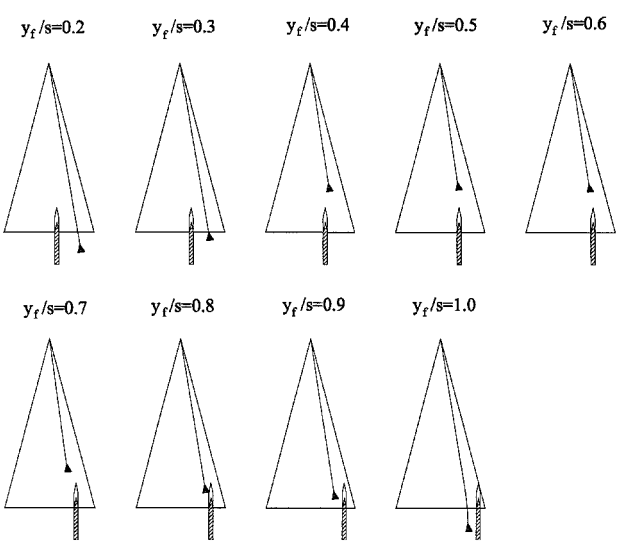

Fig. 2 Time-averaged breakdown location for no fin deflection.

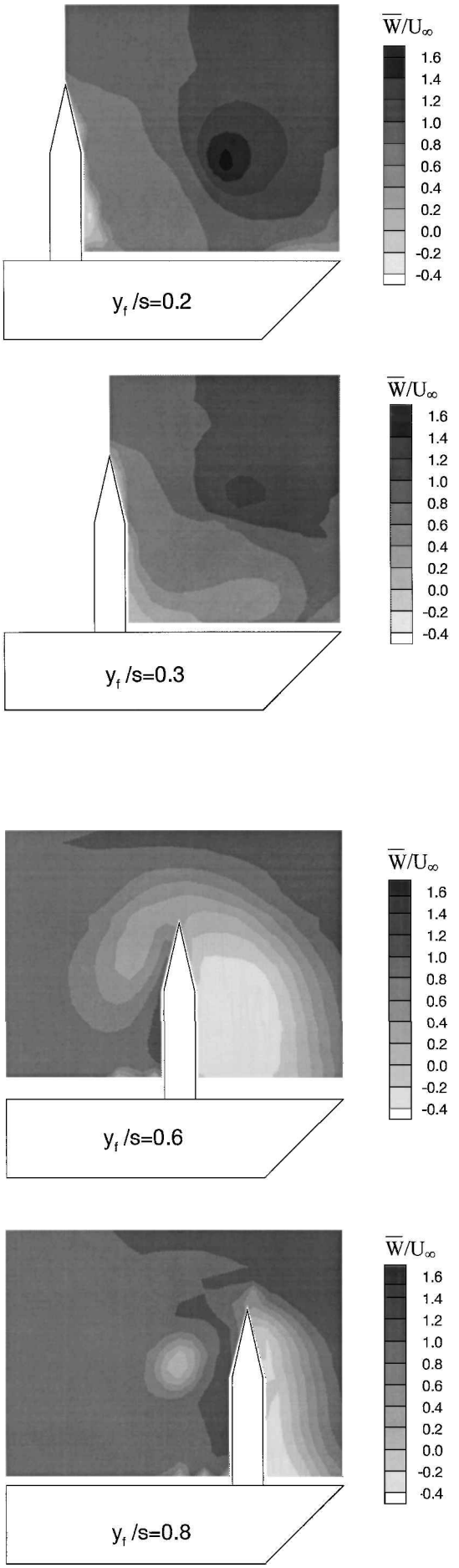

Fig. 3 Constant contours of the time-averaged streamwise velocity, $x/c = 1.0$.

Results

The angle of attack was fixed at $\alpha = 20$ deg throughout the study. Although vortex breakdown is not observed over the wing in the absence of the fin, it may move over the wing depending on the fin location y_f (see Fig. 1). The time-averaged breakdown location is shown for no fin deflection ($\phi = 0$ deg) in Fig. 2. In Fig. 2, the leading edge of the fin on the wing surface and the cross section of the fin with the vortex axis are shown with respect to the vortex breakdown location. The time-averaged breakdown location is very sensitive to the location of the fin due to the external pressure gradient set by the fin. Hall[15] showed that small external pressure gradients can be amplified along the core of the vortices, leading to a stagnation point. Thus, the large sensitivity of the vortex breakdown location to a streamwise pressure gradient along the exterior of the vortex is very much expected. It is also known that this pressure gradient is set not only by the fin geometry, but also by the flow separation region that may form over the fin.[7]

Note that the breakdown location is never steady and fluctuates in the streamwise direction. The rms value of these fluctuations varied between 1 and 2% of the wing chord length, depending on the fin location. It was around $0.01c$ when the time-averaged breakdown location was near or downstream of the fin, for example, $y_f/s = 0.3$ and 0.8. When the time-averaged breakdown location was well upstream of the fin, such as $y_f/s = 0.6$, the rms value of the fluctuations of breakdown location was around $0.02c$.

The component of flow velocity parallel to the wing surface was measured in the crossplane at the trailing edge, $x/c = 1.0$, for several cases. The constant contours of the time-averaged velocity are shown in Fig. 3 for $y_f/s = 0.2$, 0.3, 0.6, and 0.8. For $y_f/s = 0.2$, the time-averaged breakdown location is downstream of the trailing edge; therefore, a jet-like axial velocity is observed in the core of the vortex. For $y_f/s = 0.3$, the time-averaged breakdown location is just at the trailing edge. Because of the fluctuations of breakdown location in the streamwise direction, both jetlike and wakelike velocity distributions exist intermittently in the measurement plane and tend to cancel each other. Because of this, the time-averaged velocity distribution does not reveal the core of the leading-edge vortex. For $y_f/s = 0.6$, the time-averaged breakdown location is well upstream of the fin and the measurement plane. The fin appears to split the wake of the vortex breakdown. According to the measurements[16] at $x/c = 0.5$ (upstream of breakdown location), the leading-edge vortex is located at $y/s = 0.62$. Hence, the case of $y_f/s = 0.6$ represents a direct impingement of the breakdown wake on the fin. Note also, for this case, there is a large separated region between the fin and the leading edge of the wing. As mentioned before, this separated region may be important in determining the location of vortex breakdown. For $y_f/s = 0.8$, the time-averaged breakdown location is just upstream of the measurement plane. The core of the vortex is revealed by the wakelike velocity distribution. The breakdown wake seems to be displaced inboard due to the existence of the fin. Again, the flow separation between the fin and the leading edge of

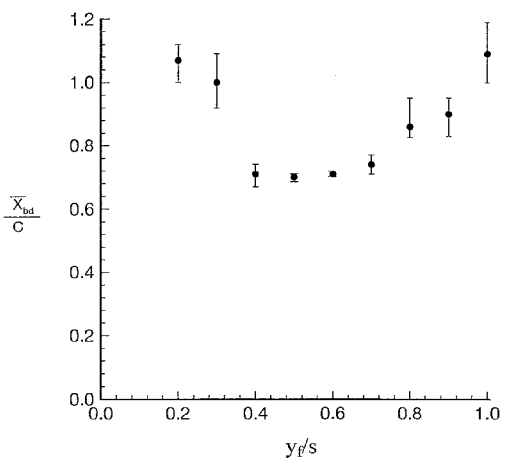

Fig. 4 Variation of time-averaged breakdown location for $\phi = 0$ deg (filled symbols) and $\phi = \pm 10$ deg (vertical bars).

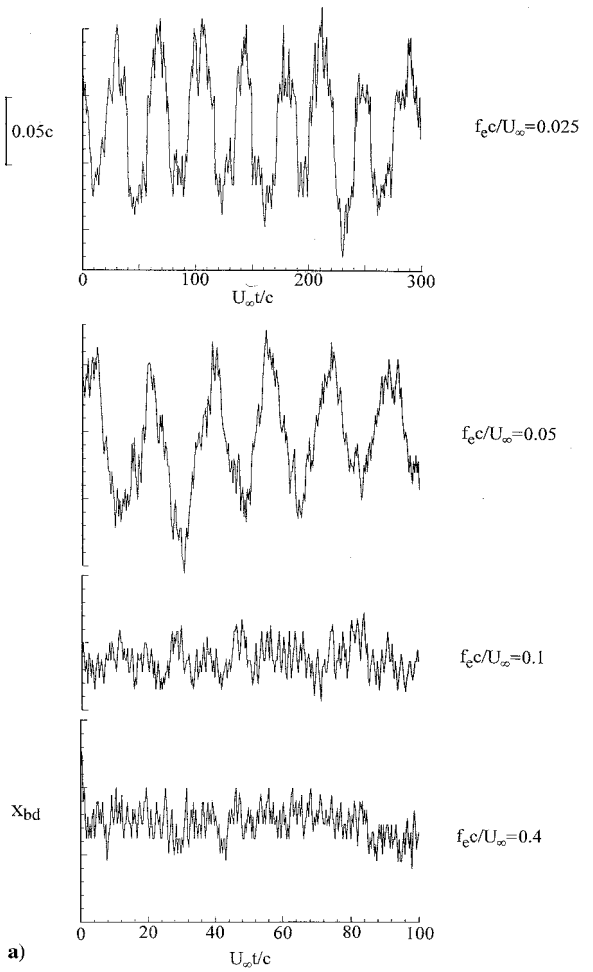

the wing is evident. In summary, the flow pattern around the fin may be very complex depending on the fin location, as illustrated in these examples. However, it will be shown later that the dynamic response of vortex breakdown location to the oscillations of the fin is very similar for all fin locations.

In Fig. 4, the time-averaged breakdown locations for $\phi = 0$ deg and for $\phi = \pm 10$ deg (as a vertical bar) are shown to demonstrate the effect of the static deflections. When the breakdown location is well upstream of the fin, it is not sensitive to the static deflections of the fin (see also Fig. 2). However, when the breakdown location is near or downstream of the fin, it is very sensitive to the static deflections of the fin. One concludes that, when the breakdown location is well upstream, the relative change in the external pressure gradient due to the fin deflection does not have much effect on breakdown. This is because a large pressure gradient has already induced premature breakdown.

Based on the results presented in Fig. 4, it was decided to study the effect of dynamic fin oscillations in detail for specific cases. Fin locations of $y_f/s = 0.2$, 0.3, and 0.8 were chosen as representative of the cases of large sensitivity of breakdown location. On the other hand, the case of $y_f/s = 0.6$ was chosen as representative of small sensitivity of breakdown location. For all cases, the amplitude of the fin oscillations was held constant at 10 deg ($\phi = \pm 10$ deg), and the excitation frequency f_e was varied. In Fig. 5, the time history of breakdown location is shown for different fin oscillation frequencies for $y_f/s = 0.2$, 0.3, and 0.8. For $y_f/s = 0.2$, it is seen that the amplitude of the fluctuations of breakdown location is very large for $f_e c/U_\infty = 0.025$ and 0.05. However, for larger frequencies, the variations of the breakdown location are much smaller. Similar observations can be made for $y_f/s = 0.3$ and 0.8. For $f_e c/U_\infty = 0.025$ and 0.05, the periodic response of breakdown location with large amplitude is common. The variation of breakdown location is more or less locked to the fin motion. For $f_e c/U_\infty = 0.10$, it is still possible to observe the quasi-periodic nature of breakdown location, although the amplitude is smaller. For $f_e c/U_\infty = 0.40$, vortex breakdown does not respond much to fin oscillations. These results clearly

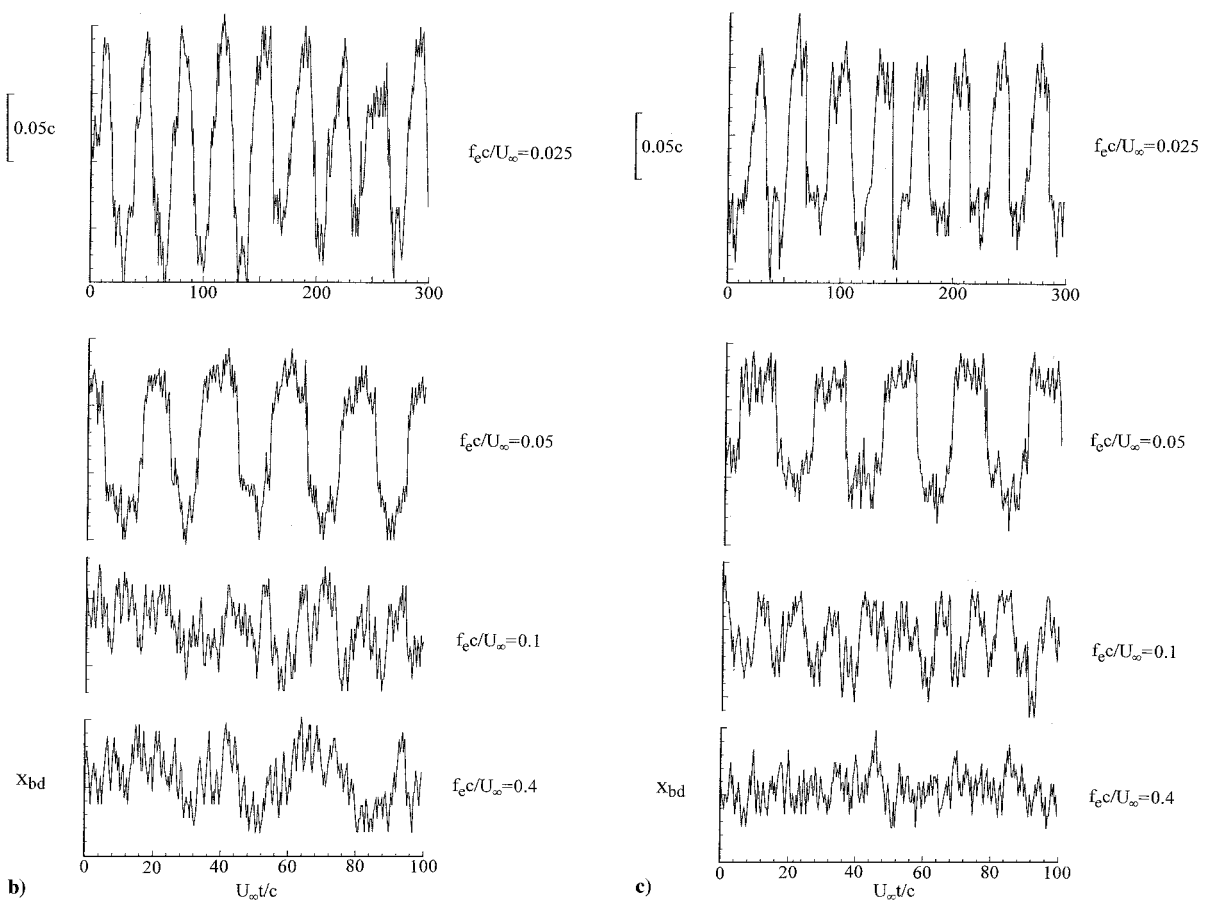

Fig. 5 Time histories of breakdown location for different fin oscillation frequencies for a) $y_f/s = 0.2$, b) $y_f/s = 0.3$, and c) $y_f/s = 0.8$.

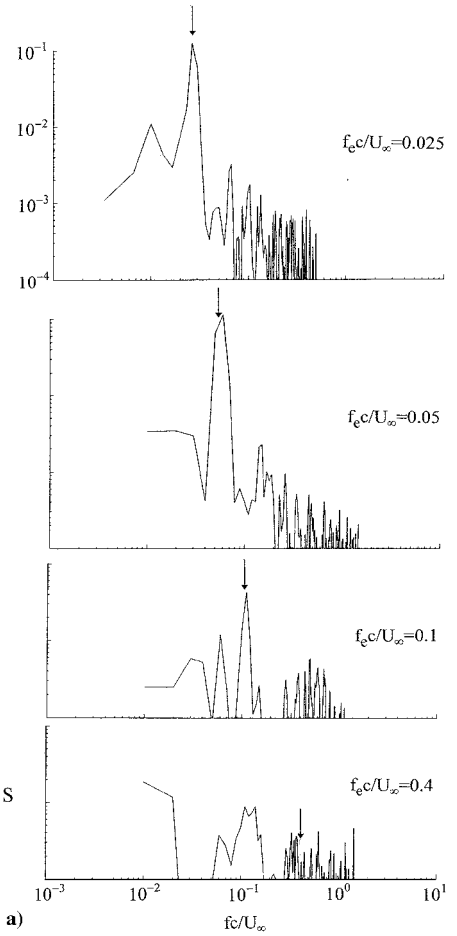

show that the effect of the fin oscillations on vortex breakdown may be important, depending on the frequency of the oscillations.

The effect of the excitation frequency can also be seen from the spectra of breakdown location shown in Fig. 6. In each spectrum, the excitation or forcing frequency is shown with an arrow. For frequencies of $f_ec/U_\infty = 0.025$, 0.05, and 0.1, a large spectral amplitude is observed at the excitation frequency. The peak spectral amplitude decreases with increasing excitation frequency. For $f_ec/U_\infty = 0.40$, the spectral amplitude at the forcing frequency is very small. These results suggest that the response of breakdown location to an oscillating fin is similar to the effect of a low-pass filter. These observations were common regardless of the location of the fin. This may be very important for fin buffeting problems. For example, if the cutoff frequency is known, lower frequencies may be avoided by proper design of the fin.

As discussed earlier, the case of $y_f/s = 0.6$ was very different because of almost no sensitivity of breakdown location to the static deflections of the fin. In Fig. 7, the time history of breakdown location is shown for several fin oscillation frequencies. The overall amplitude of the fluctuations does not change much. The rms value of the fluctuations is around $0.02c$. Nevertheless, in certain cases, such as $f_ec/U_\infty = 0.1$, a quasi-periodic behavior is observed in the time history of breakdown location. In fact, the spectra shown in Fig. 8 reveal that, at low frequencies, there is a spectral peak at the excitation frequency. However, for $f_ec/U_\infty = 0.40$ and 1.0, the spectral amplitude at the excitation frequency vanishes, while some low-frequency components are observed. Again, one concludes that the response is like a low-pass filter because the vortex breakdown does not respond to high-frequency oscillations. Hence, with regard to the effect of excitation frequency, the response of breakdown in this case ($y_f/s = 0.6$) is similar to the other cases ($y_f/s = 0.2$, 0.3, and 0.8) where the breakdown location is much more sensitive.

For the cases of $y_f/s = 0.2$, 0.3, and 0.8, the rms value of the fluctuations strongly depends on the excitation frequency. This is

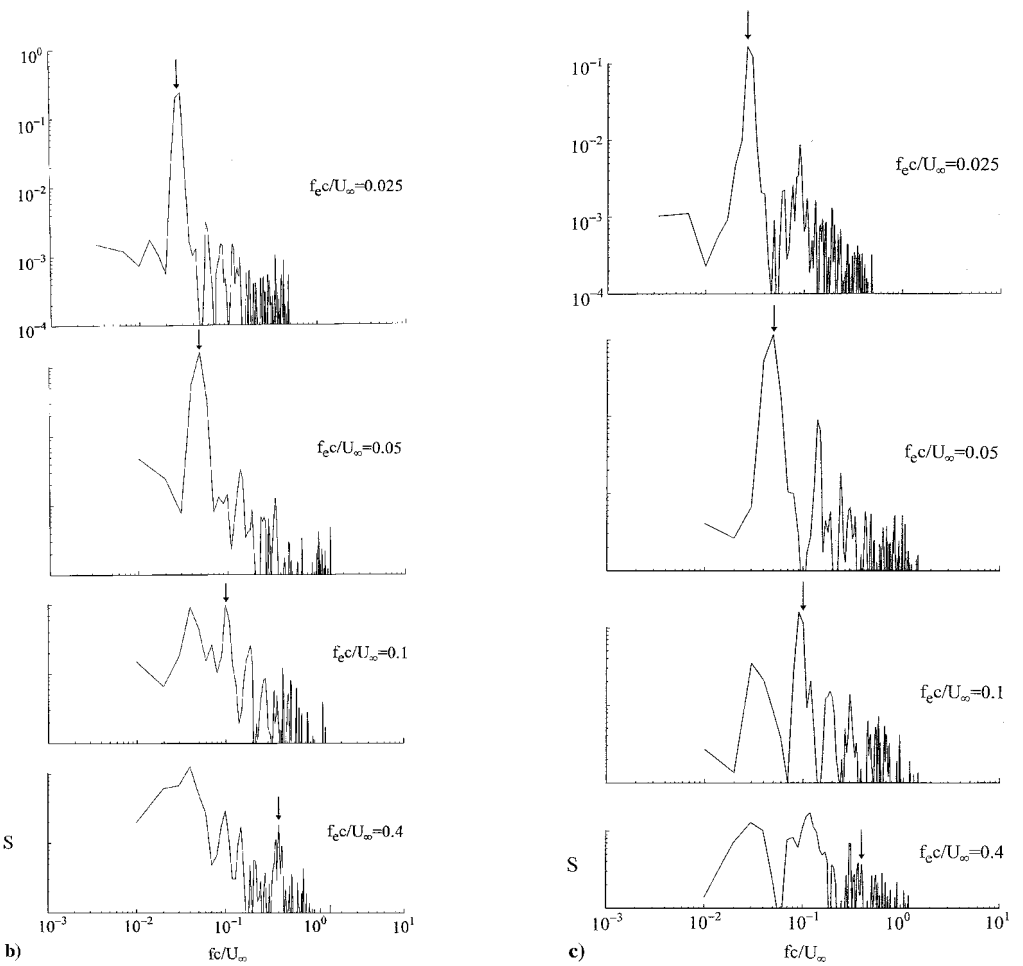

Fig. 6 Spectra of breakdown location for different fin oscillation frequencies for a) $y_f/s = 0.2$, b) $y_f/s = 0.3$, and c) $y_f/s = 0.8$.

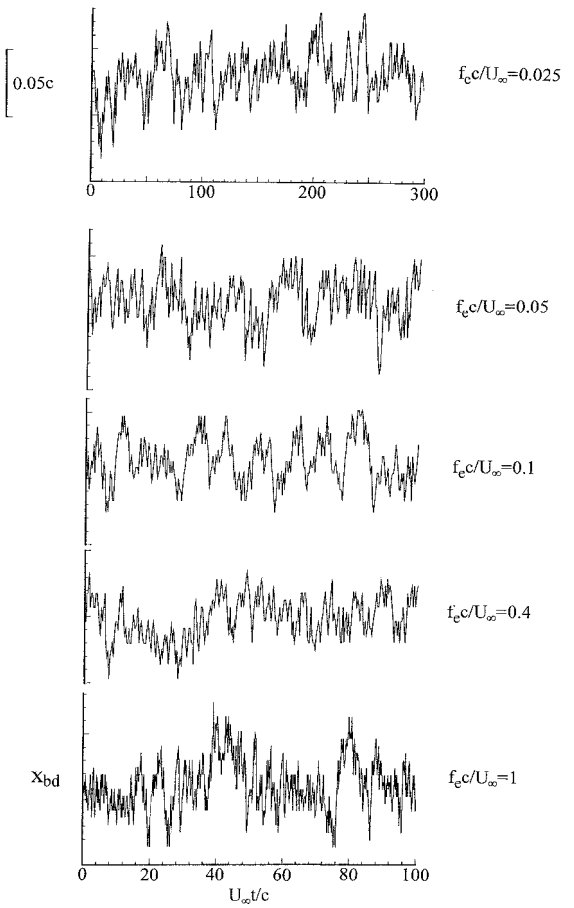

Fig. 7 Time histories of breakdown location for different fin oscillation frequencies for $y_f/s = 0.6$.

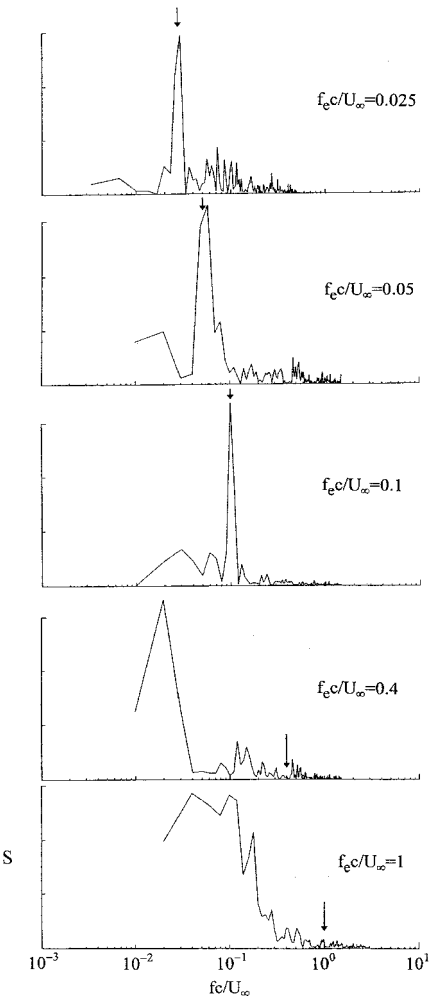

Fig. 8 Spectra of breakdown location for different fin oscillation frequencies for $y_f/s = 0.6$.

evident from the time histories shown in Fig. 5. Whereas the largest rms value is close to $0.06c$, it decreases very quickly to the levels observed for no oscillations (about $0.01c$) as the frequency is increased. Obviously, the largest rms value depends on the sensitivity of breakdown location in the case of static fin deflection. Therefore, the amplitude ratio was defined as the ratio of the rms value of the fluctuations of breakdown location to its quasi-steady counterpart. The latter was calculated from the data shown in Fig. 4, assuming that the time variation of breakdown location is a harmonic function, and therefore the rms value in the quasi-steady case is $0.707A$, where $2A$ is the peak-to-peak variation (corresponding to $\phi = \pm 10$ deg). The amplitude ratio as a function of dimensionless frequency is shown in Fig. 9 for $y_f/s = 0.2$, 0.3, and 0.8. It is seen that the amplitude ratio decreases with increasing frequency, and the amplitude attenuation is similar to that of a low-pass filter.

Note that this type of frequency response is observed for the amplitude of the variations of breakdown location in other unsteady flows regardless of the type of unsteady motion. For example, for pitching motion of delta wings, the amplitude of breakdown location decreases with forcing frequency. This effect appears in the form of a flattening of the hysteresis loops with increasing frequency. This together with other observations of vortex breakdown location (such as phase lag) suggest that the response of breakdown location is similar to that of a first-order system. With this idealization, the time constant was estimated from the time history of breakdown location in response to a given unsteady wing/surface motion.[17,18] The normalized time constant $\tau U_\infty/c$ is on the order of unity. By curve fitting to a large database (taken from many studies published in the literature), Greenwell and Wood[18] obtained $\tau U_\infty/c = 1.67$. The amplitude ratio (AR) for a first-order system can be written as

$$\mathrm{AR} = 1/\sqrt{1 + (\omega\tau)^2} \tag{1}$$

or

$$\mathrm{AR} = 1\Big/\sqrt{1 + \left(\frac{2\pi f c}{U_\infty}\frac{\tau U_\infty}{c}\right)^2} \tag{2}$$

Using $\tau U_\infty/c = 1.67$, one obtains

$$\mathrm{AR} = 1/\sqrt{1 + (10.49 f c/U_\infty)^2} \tag{3}$$

which is plotted in Fig. 9. Note that this curve represents a curve fit to the data with large scatter. It is seen from Fig. 9 that the amplitude attenuation for pitching wings reasonably agrees with the results for the oscillating fin. This suggests that the decrease of the amplitude with frequency is due to a common, universal mechanism, regardless of the unsteady motion. A proposed mechanism will be presented in the next section.

Discussion

As suggested in the Introduction, the wave propagation characteristics of the flow may offer an explanation of the experimental results. It is well known that waves may propagate upstream through the vortex core with a certain phase speed.[14] If the disturbances are in the form of $\exp[i(kx - \omega t - n\theta)]$, the phase speed of a wave is $c = \omega/k$. Benjamin[19] considered the propagation of axisymmetric $n = 0$ waves on a columnar vortex in the long-wave limit, $k \to 0$. If the phase speed is negative, the time-averaged flow is subcritical, and the disturbances can propagate upstream. Otherwise, the flow is called supercritical. According to the calculations for experimentally measured profiles, the flows upstream of breakdown location, which have jetlike axial velocity profiles, are supercritical.[14] The measured flows downstream of breakdown location, which have

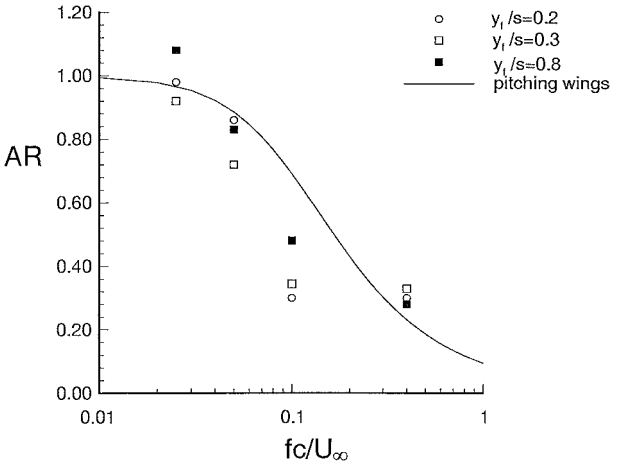

Fig. 9 Variation of the AR as a function of forcing frequency.

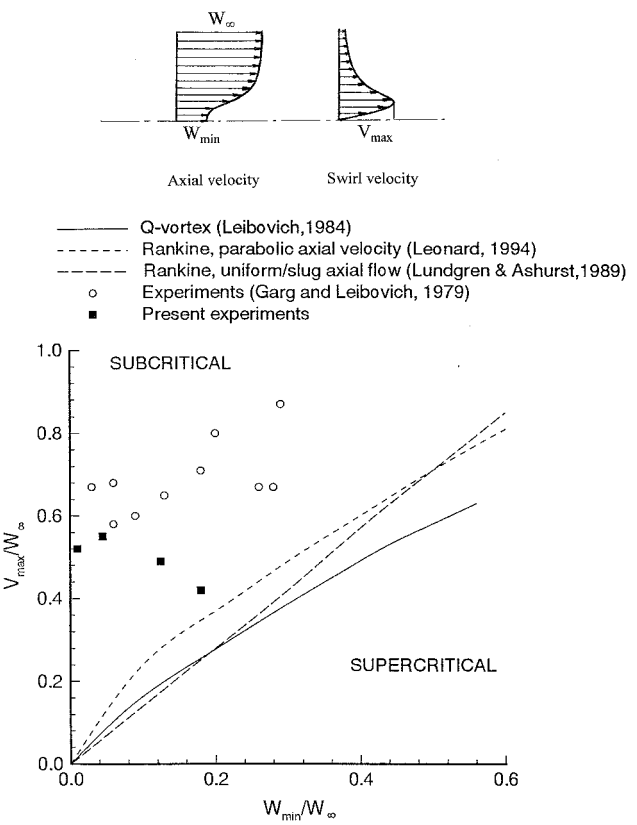

Fig. 10 Parameter space for several vortex models, showing the regions of subcritical and supercritical flow and data from previous work and present investigation.

wakelike axial velocity profiles, are subcritical. Leibovich[14] calculated the regions of subcritical and supercritical flow for the Q vortex whose velocity profiles may be given by

$$W(r) = W_\infty + (W_{\min} - W_\infty)\exp(-r^2)$$
$$V(r) = 1.57V_{\max}(1/r)[1 - \exp(-r^2)] \qquad (4)$$

As shown in Fig. 10, whether the flow is subcritical or supercritical depends on the ratios $W_{\min}/W_\infty$ and $V_{\max}/W_\infty$. It is also seen that the experimentally measured profiles[20] in a vortex tube are subcritical. In Fig. 10, two other curves indicating the regions of subcritical and supercritical flow are shown. Leonard[21] calculated the phase speed for a Rankine vortex with parabolic jetlike axial velocity profile. After a simple Galilean transformation, the phase speed of upstream propagating waves, in the limit of zero wave number, can be found.[22] To have a subcritical flow, the phase speed c should be negative, $c < 0$. This condition provides the region of subcritical flow as a function of $W_{\min}/W_\infty$ and $V_{\max}/W_\infty$, as shown in Fig. 10. Lundgren and Ashurst[23] calculated the phase speed for a Rankine vortex with uniform (slug) axial flow. After a simple Galilean transformation, the phase speed of upstream propagating waves can be found.[22] The condition of $c < 0$ is shown in Fig. 10. The three curves showing the regions of subcritical and supercritical flows are not very different, suggesting only a weak dependence on the details of the swirl and axial profiles.

Also shown in Fig. 10 are the values of $W_{\min}/W_\infty$ and $V_{\max}/W_\infty$ from the measured velocity profiles downstream of breakdown location in this investigation for $y_f/s = 0.3$ and 0.6. The data point with the smallest $W_{\min}/W_\infty$ is for $\Delta x/c = 0.15$ (where Δx represents the distance from the time-averaged breakdown location) and $y_f/s = 0.6$. The other three data points are for $\Delta x/c = 0.15, 0.2$, and 0.3 in increasing order of $W_{\min}/W_\infty$ for $y_f/s = 0.3$. The axial and swirl velocity profiles are given in Ref. 22 in detail. For distances $\Delta x/c \geq 0.15$, a wakelike velocity is observed (with positive velocity everywhere), whereas reversed flow is evident for $\Delta x/c = 0.10$. The data presented in Fig. 10 do not include data from profiles with reversed axial velocity. The asymmetries, particularly in the swirl velocity component, are common due to the existence of the fin. To take the asymmetry into account, average values were used in Fig. 10. Note that, in all cases, the flow is subcritical. Also, the vortices formed over delta wings are weaker compared to those generated in vortex-tube experiments.

Leibovich[14] points out that the ability of disturbances to propagate upstream is determined by the group velocity $C_g = \partial\omega/\partial k$, not the phase velocity. However, he shows that, because $C_g \to c$ as $k \to 0$ flows that are subcritical based on a phase velocity criterion are also subcritical based on the group velocity criterion. The regions of subcritical and supercritical flows shown in Fig. 10 are valid in the limit of $k \to 0$. For an oscillating fin, the wave propagation characteristics of the flow as a function of forcing frequency are important. Tsai and Widnall[24] applied a linear wave propagation analysis to obtain the dispersion relation $\omega = \omega(k)$ and the group velocity $C_g = \partial\omega/\partial k$ for the velocity profiles measured by Garg and Leibovich[20] downstream of vortex breakdown (also shown in Fig. 10). Results from sample calculations for three selected profiles designated A, B, and C are shown in Fig. 11. The velocity ratios ($W_{\min}/W_\infty$, $V_{\max}/W_\infty$) are (0.03, 0.67), (0.18, 0.71), and (0.28, 0.67) for A, B, and C, respectively. In Fig. 11, the normalized group velocity C_g/W_∞ is shown as a function of wave number k. At low wave numbers, the flow is always subcritical. With increasing wave number k, the magnitude of the group velocity decreases to near zero, and the flow may even become supercritical. In all examples presented by Tsai and Widnall,[24] this trend is observed. This means that the ability of disturbances to propagate upstream decreases with increasing wave number (or frequency). This qualitatively explains our observations of the response of breakdown location as the forcing frequency is varied. However, a direct application of these calculations to our problem is not possible because the results are specific to the velocity profiles.

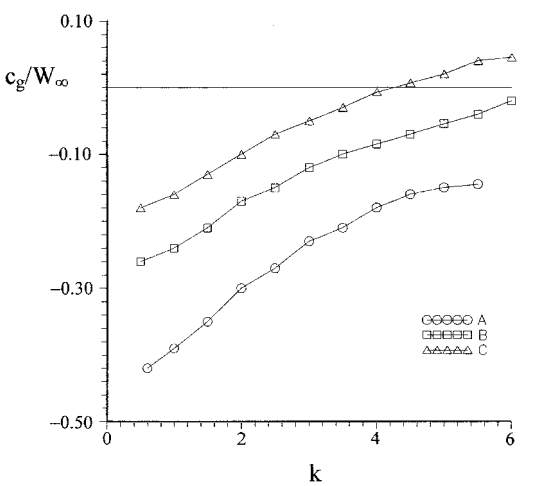

Fig. 11 Normalized group velocity as a function of wave number.

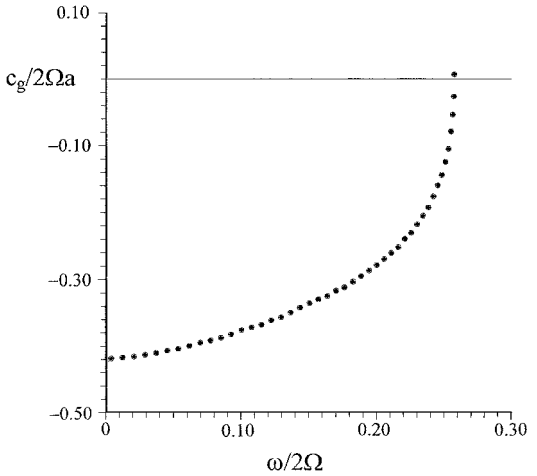

Fig. 12 Normalized group velocity as a function of $\omega/2\Omega$.

The effect of forcing frequency on the wave propagation characteristics of the flow can also be seen from a simple vortex model. We consider a cylindrical vortex with the Rankine velocity distribution

$$V(r) = \Omega r \quad \text{for} \quad r \le a, \qquad V(r) = \Omega a^2/r \quad \text{for} \quad r \ge a \tag{5}$$

and no axial velocity. The exact dispersion equation was determined by Kelvin (for example, see Maxworthy[25]) for axisymmetric disturbances as

$$\frac{1}{\beta a}\frac{J_0'(\beta a)}{J_0(\beta a)} = -\frac{1}{ka}\frac{K_0'(ka)}{K_0(ka)} \tag{6}$$

where $\beta^2 = k^2[4\Omega^2 - \omega^2]/\omega^2$ and J_0 and K_0 are Bessel functions. The relation $\omega = \omega(k)$ was found numerically, and the group velocity was calculated as $C_g = \partial\omega/\partial k$. The normalized group velocity $C_g/2\Omega a$ is shown as a function of $\omega/2\Omega$ in Fig. 12. For comparison, the dispersion relation in the long-wave limit ($k \to 0$) is given by

$$\omega = C_0 k[1 + 0.1729(ka)^2\, \ell n(ka/2) + \mathcal{O}(k^2a^2)] \tag{7}$$

where $C_0 = -0.416$ (2Ωa); hence, $C_{g0} = -0.416$ ($2\Omega a$) as $k \to 0$. The numerical solution of the dispersion relation provided $C_{g0} = -0.418$ ($2\Omega a$). It is seen from Fig. 12 that the magnitude of the group velocity decreases very rapidly with increasing frequency. The disturbances with frequencies larger than $\omega/2\Omega \cong 0.26$ will not propagate upstream according to this simple model. This is similar to our experimental findings regarding the response of breakdown location. Between $fc/U_\infty = 0.1$ and 0.4, the response diminishes very quickly. In fact, a quantitative estimate of the cutoff frequency can be made by estimating Ω from the measured velocity profiles. Using the data given in Ref. 22, one can calculate Ω as $V_{\max}/a$, where $V_{\max}$ is the maximum swirl velocity and a is the radial distance at which $V_{\max}$ is observed. The calculated values varied from $\Omega = 7U_\infty/c$ to $10U_\infty/c$. Also, comparisons were made with the velocity measurements[26–29] made downstream of breakdown location in the absence of a fin. Estimates of Ω from these results varied between $7U_\infty/c$ and $14U_\infty/c$. If an average value of $\Omega = 10U_\infty/c$ is used, the theoretical cutoff frequency can be estimated from $\omega/2\Omega = 0.26$, which provides $\omega = 5.2\ U_\infty/c$. Using $\omega = 2\pi f$, one obtains $fc/U_\infty = 0.83$. Because the experimental cutoff frequency is around $fc/U_\infty = 0.40$, it is concluded that this rough estimate, which is valid for a very simplified vortex model, provides a reasonable order of magnitude estimate for the cutoff frequency.

Conclusions

The effect of aeroelastic deflections of a fin on vortex breakdown phenomenon was investigated in a water tunnel. Aeroelastic deflections of the fin in the first bending mode were simulated by forced oscillations of a rigid fin. The frequency of the fin oscillations was varied, and the interaction of vortex breakdown with the oscillating fin was investigated by flow visualization and LDV measurements.

Experiments were conducted for a leading-edge vortex generated by a $\Lambda = 75$ deg sweep delta wing at an angle of attack $\alpha = 20$ deg. Although vortex breakdown is not observed over the wing in the absence of the fin, it may move over the wing depending on the fin location y_f. The time-averaged breakdown location for no fin oscillations as well as the sensitivity of breakdown location to static fin deflections strongly depend on the fin location. For fin oscillations, time histories and spectra show the quasi-periodic response of breakdown location for low frequencies. The amplitude of the variations of breakdown location becomes smaller with increasing frequency. At high frequencies, vortex breakdown does not respond to fin oscillations. For frequencies higher than a cutoff frequency (around $fc/U_\infty \approx 0.40$), the spectra reveal that the spectral peak at the forcing frequency vanishes. Both the frequency response and the amplitude attenuation suggest that the response of breakdown location to an oscillating fin is similar to that of a low-pass filter. This result may be very important for fin buffeting problems. For example, because the cutoff frequency is known, lower natural frequencies may be avoided by proper design of the fin. The results were similar regardless of the location of the fin. It was also suggested that the dynamic response of vortex breakdown location is similar in other unsteady flows regardless of the type of unsteady motion. In particular, it was shown that the amplitude response is very similar for pitching delta wings and oscillating fins. This suggests that there exists a common, universal mechanism regardless of the unsteady motion. A proposed mechanism based on the wave propagation characteristics of the vortex flows was presented. It is based on the concept of subcritical flow that exists downstream of breakdown location. Disturbances due to fin deflections may propagate upstream, and the group velocity of the disturbances depends on the axial wave number. It was shown that the ability of disturbances to propagate upstream decreases with increasing wave number (or frequency). A simple model predicts that the disturbances with frequencies higher than a cutoff frequency will not propagate upstream, which agrees very well with the experimental observations.

Acknowledgments

This material is based on work supported by the European Office of Aerospace Research and Development, U.S. Air Force Office of Scientific Research, and U.S. Air Force Research Laboratory, under Contract F61775-99-WE013.

References

[1]Gursul, I., and Xie, W., "Buffeting Flows over Delta Wings," *AIAA Journal*, Vol. 37, No. 1, 1999, pp. 58–65.

[2]Gursul, I., "Unsteady Flow Phenomena over Delta Wings at High Angle of Attack," *AIAA Journal*, Vol. 32, No. 2, 1994, pp. 225–231.

[3]Gursul, I., and Yang, H., "On Fluctuations of Vortex Breakdown Location," *Physics of Fluids*, Vol. 7, No. 1, 1995, pp. 229–231.

[4]Mayori, A., and Rockwell, D., "Interaction of a Streamwise Vortex with a Thin Plate: A Source of Turbulent Buffeting," *AIAA Journal*, Vol. 32, No. 10, 1994, pp. 2022–2029.

[5]Wolfe, S., Lin, J. C., and Rockwell, D., "Buffeting at the Leading-Edge of a Flat Plate Due to a Streamwise Vortex: Flow Structure and Surface Pressure Loading," *Journal of Fluids and Structures*, Vol. 9, 1995, pp. 359–370.

[6]Canbazoglu, S., Lin, J. C., Wolfe, S., and Rockwell, D., "Buffeting of Fins: Distortion of Incident Vortex," *AIAA Journal*, Vol. 33, No. 11, 1995, pp. 2144–2150.

[7]Gordnier, R. E., and Visbal, M. R., "Numerical Simulation of the Impingement of a Streamwise Vortex on a Plate," AIAA Paper 97-1781, June–July 1997.

[8]Patel, M. H., and Hancock, G. J., "Some Experimental Results of the Effect of a Streamwise Vortex on a Two-Dimensional Wing," *Aeronautical Journal*, April 1974, pp. 151–155.

[9]Lee, B. H. K., and Brown, D., "Wind-Tunnel Studies of F/A-18 Tail Buffet," *Journal of Aircraft*, Vol. 24, No. 1, 1992, pp. 146–152.

[10]Washburn, A. E., Jenkins, L. N., and Ferman, M. A., "Experimental Investigation of Vortex–Fin Interaction," AIAA Paper 93-0050, Jan. 1993.

[11]Meyn, L. A., and James, K. D., "Full Scale Wind Tunnel Studies of F/A-18 Tail Buffet," AIAA Paper 93-3519, 1993.

[12]Lee, B. H. K., and Tang, F. C., "Characteristics of the Surface Pressures on a F/A-18 Vertical Fin Due to Buffet," *Journal of Aircraft*, Vol. 31, No. 1, 1994, pp. 228–235.

[13]Bean, D. E., and Wood, N. J., "Experimental Investigation of Twin-Fin Buffeting and Suppression," *Journal of Aircraft*, Vol. 33, No. 4, 1996, pp. 761–767.

[14]Leibovich, S., "Vortex Stability and Breakdown: Survey and Extension," *AIAA Journal*, Vol. 22, No. 9, 1984, pp. 1192–1206.

[15]Hall, M. G., "Vortex Breakdown," *Annual Review of Fluid Mechanics*, Vol. 4, 1972, pp. 195–218.

[16]Xie, W., "An Experimental Investigation of Buffeting Flows over Delta Wings," M.S. Thesis, Dept. of Mechanical, Industrial, and Nuclear Engineering, Univ. of Cincinnati, Cincinnati, OH, Dec. 1998.

[17]Srinivas, S., Gursul, I., and Batta, G., "Active Control of Vortex Breakdown Over Delta Wings," AIAA Paper 94-2215, June 1994.

[18]Greenwell, D. I., and Wood, N. J., "Some Observations on the Dynamic Response to Wing Motion of the Vortex Burst Phenomenon," *Aeronautical Journal*, Feb. 1994, pp. 49–59.

[19]Benjamin, T. B., "Theory of the Vortex Breakdown Phenomenon," *Journal of Fluid Mechanics*, Vol. 14, 1962, pp. 593–629.

[20]Garg, A. K., and Leibovich, S., "Spectral Characteristics of Vortex Breakdown Flowfields," *Physics of Fluids*, Vol. 22, No. 11, 1979, pp. 2053–2064.

[21]Leonard, A., "Nonlocal Theory of Aera-Varying Waves on Axisymmetric Vortex Tubes," *Physics of Fluids*, Vol. 6, No. 2, 1994, pp. 765–777.

[22]Gursul, I., and Xie, W., "Interaction of Vortex Breakdown with an Oscillating Fin," AIAA Paper 2000-0279, Jan. 2000.

[23]Lundgren, T. S., and Ashurst, W. T., "Area-Varying Waves on Curved Vortex Tubes With Application to Vortex Breakdown," *Journal of Fluid Mechanics*, Vol. 200, 1989, pp. 283–307.

[24]Tsai, C.-Y., and Widnall, S. E., "Examination of Group-Velocity Criterion for Breakdown of Vortex Flow in a Divergent Duct," *Physics of Fluids*, Vol. 23, No. 5, 1980, pp. 864–870.

[25]Maxworthy, T., "Waves on Vortex Cores," *Fluid Dynamics Research*, Vol. 3, 1988, pp. 52–62.

[26]Schmucker, A., and Gersten, K., "Vortex Breakdown and its Control on Delta Wings," *Fluid Dynamic Research*, Vol. 3, 1988, pp. 268–272.

[27]Payne, F. M., Ng, T. T., and Nelson, R. C., "Seven Hole Probe Measurement of Leading Edge Vortex Flows," *Experiments in Fluids*, Vol. 7, 1989, pp. 1–8.

[28]Roos, F. W., and Kegelman, J. T., "Recent Explorations of Leading-Edge Vortex Flowfields," NASA High-Angle-of-Attack Technology Conf., NASA Langley Research Center, Hampton, VA, Oct.–Nov. 1990.

[29]McCormick, S., and Gursul, I., "Effect of Shear Layer Control on Leading Edge Vortices," AIAA Paper 96-0541, Jan. 1996.

M. Samimy
Associate Editor